Univerza
v Ljubljani
Fakulteta
za gradbeništvo
in geodezijo

Jamova cesta 2
1000 Ljubljana, Slovenija
http://www3.fgg.uni-lj.si/

University
of Ljubljana
Faculty of
Civil and Geodetic
Engineering

Jamova cesta 2
SI – 1000 Ljubljana, Slovenia
http://www3.fgg.uni-lj.si/en/

Vrankar, L., Libre, N. A., Ling, L., Turk, G., Runovc, F. 2013. Solving moving-boundary problems with the wavelet adaptive radial basis functions method. *Computers & Fluids* 86: 37–44.
DOI: 10.1016/j.compfluid.2013.06.029

Solving Moving-Boundary Problems with the Wavelet Adaptive Radial Basis Functions Method

Leopold Vrankar[a,*], Nicolas Ali Libre[b], Leevan Ling[b], Goran Turk[c], Franc Runovc[a]

[a] *University of Ljubljana, Faculty of Natural Sciences and Engineering, Aškerčeva cesta 12, Ljubljana, Slovenia*
[b] *Department of Mathematics, Hong Kong Baptist University, Hong Kong*
[c] *University of Ljubljana, Faculty of Civil and Geodetic Engineering, Jamova cesta 2, Ljubljana, Slovenia*

Abstract

Moving boundaries are associated with the time-dependent problems where the momentary position of boundaries needs to be determined as a function of time. The level set method has become an effective tool for tracking, modelling and simulating the motion of free boundaries in fluid mechanics, computer animation and image processing. This work extends our earlier work on solving moving boundary problems with adaptive meshless methods. In particular, the objective of this paper is to investigate numerical performance the radial basis functions (RBFs) methods, with compactly supported basis and with global basis, coupled with a wavelet node refinement technique and a greedy trial space selection technique. Numerical simulations are provided to verify the effectiveness and robustness of RBFs methods with different adaptive techniques.

Key words: moving-boundary problems, wavelet method, level set method, global RBFs, compactly supported RBFs, partial differential equations, adaptive greedy algorithm

*Corresponding author:

E-mail addresses: leopold.vrankar@gmail.com

1. Introduction

One common feature of moving-boundary problems is the fact that the location of the solid-liquid interface is not known in advance and has to be determined during the analysis. Moving boundary problems can be considered as time-dependent problem where the position of the boundary has to be determined as a function of time.

Various numerical methods are known to solve the moving-boundary problems, e.g. front-tracking, front-fixing, and fixed-domain methods [1]. The Level Set Methods (LSM) have become an effective tool for simulating the motion of free boundaries in fluid mechanics and other similar processes [2–7]. The governing equation of LSM are usually solved by conventional numerical methods e.g. the finite-difference methods and the finite-element method [8, 9]. More and more attention has been given to the development of meshless methods using radial basis functions (RBFs) for the numerical solution of PDEs [10]. Recently, the RBF based meshless method has been successfully used for the numerical solution of moving boundary problems [11].

Adaptive techniques could be used to improve the efficiency of numerical methods especially in LSM moving boundary problems in which the level set function should be accurately captured *only* near the zero contour. The computational resolution should be adaptively refined near the boundaries and could be coarsened elsewhere. Any adaptive technique that is employed in moving boundary problems should be fast enough as the boundary evolves with time and the location of the zero contour has to be updated at certain time steps. In recent years, wavelet methods have been used for signal processing and mathematical analysis. In this paper, we propose a wavelet-based adaptive scheme that utilizes the well-known RBFs (e.g. the multiquadrics and the Wendland's compactly supported basis) as the basis of the solution space.

The objective of this paper is to improve the resolutions, hence accuracy, of the meshless RBF method with some adaptive wavelet-greedy techniques to construct a more efficient approach for moving boundary problems. Numerical simulations are performed to verify the capability of the proposed numerical scheme in the moving boundary problems.

2. Governing equations and discretization

The level set method (LSM) is a numerical technique for tracking different types of interfaces. The advantage of the LSM is that numerical computations involving curves and surfaces can be executed on fixed Cartesian grid. Therefore, the parametrization of the object is not needed [12].

In two dimensions, the LSM represents a closed curve in the plane as the zero value of the two-dimensional auxiliary function $\Phi(\mathbf{x}, t)$, mapping $\mathbb{R}^2 \times \mathbb{R} \to \mathbb{R}$, where $\mathbf{x}$ is a position of the interface and t is a moment in time. The closed curve is presented as:

$$\Gamma = \{(\mathbf{x}, t)|\ \Phi(\mathbf{x}, t) = 0\}. \tag{1}$$

The function Φ is termed a level set function and it is assumed to take positive values inside the region delimited by the curve Γ and to take negative values elsewhere [2, 3]. The level set function is defined as a signed distance function from the interface. The moving interface at given time t is determined by locating the set of $\Gamma(t)$ for which Φ vanishes. The movement of the level set function is described as

$$\frac{\partial \Phi}{\partial t} + \mathbf{v}^T \nabla \Phi = 0, \quad \Phi(\mathbf{x}, 0) = \Phi_0(\mathbf{x}), \tag{2}$$

where $\Phi_0(\mathbf{x})$ represents the initial position of the interface and $\mathbf{v}^T = [\nu_1, \nu_2]$ is the continuous field depending on position $\mathbf{x}$.

Suppose the time derivative is discretized by an implicit scheme then we have

$$\frac{\Phi^{n+1} - \Phi^n}{\triangle t} + \nu_1 \frac{\partial \Phi^{n+1}}{\partial x} + \nu_2 \frac{\partial \Phi^{n+1}}{\partial y} = 0, \tag{3}$$

where $t_k = k \triangle t$ $\Phi^k = \Phi^k(\mathbf{x})$ is the level set variable at time t_k ($k = 0, 1, 2, \ldots$). For spatial discretization, the function Φ^k is approximated by a linear combination of radial basis functions:

$$\Phi^k(\mathbf{x}) = \sum_{j=1}^{N} \alpha_j^k \varphi_j(\mathbf{x}) = \sum_{j=1}^{N} \alpha_j^k \varphi(||\mathbf{x} - \boldsymbol{\xi}_j||), \tag{4}$$

where $\varphi_j(\mathbf{x}) := \varphi(||\mathbf{x} - \boldsymbol{\xi}_j||)$ is any radial basis function whose value depends only on the distance between $\mathbf{x}$ and a fixed set of center points $\boldsymbol{\Xi} = \{\boldsymbol{\xi}_\mathbf{1}, \ldots, \boldsymbol{\xi}_\mathbf{N}\}$

specifying the centers of RBFs and $\alpha_j(t_k)$ is the weight of the radial basis function positioned at the j^{th} center. Note that the exact positions of centers $\boldsymbol{\Xi}$ are totally arbitrary. In this paper, the centers will be adaptively placed so that their density is higher near the zero contour of Φ. On these centers, two commonly used radial basis functions, namely the globally supported *multiquadrics* $\varphi(r) = \sqrt{r^2 + c^2}$ and a *Wendland's compactly supported basis* [13] $\varphi(r) = (1-r)_+^8(32r^3 + 25r^2 + 8r + 1)$, will be used as trial functions.

Now, the initial set of weights $\alpha_j(t_0)$ is obtained from the given initial conditions. Thereafter, if we impose collocation condition also at the set of centers $\boldsymbol{\Xi}$, it is straightforward to obtain the following linear system of equations

$$\sum_{j=1}^{N} \left(\frac{\varphi_j(\boldsymbol{\xi}_i)}{\triangle t} + \nu_1 \frac{\partial \varphi_j(\boldsymbol{\xi}_i)}{\partial x} + \nu_2 \frac{\partial \varphi_j(\boldsymbol{\xi}_i)}{\partial y} \right) \alpha_j^{k+1} = \frac{\Phi^k(\boldsymbol{\xi}_j)}{\triangle t} \quad i = 1, ..., N. \tag{5}$$

which allows us to update $\{\alpha_j^k\}$ to $\{\alpha_j^{k+1}\}$ $(k = 0, 1, 2, \ldots)$. The presented material to this point is standard; readers can find out more implementation details in [11].

3. Adaptive placement of "centers"

As mentioned, the zero contour of Φ is what we are interested in. The first adaptive technique is wavelet-based technique that make our RBF centers $\boldsymbol{\Xi}$, which are also taken as the set of collocation points, with higher density around the zero contour. Intuitively, more collocations or data means more information that will allow us to better capture the details of the contour curve.

In recent years, some attempts have been made to relate the RBFs to wavelets. The concept of wavelet analysis was introduced in applied mathematics by the end of the 1980s by Daubechies [14]. Since then interest has grown rapidly in developing wavelet applications in engineering and science. Recently, the wavelet analysis has been used in RBF collocation method to adaptively refine mesh in regions with localized features [15–17]. The advantage of the adaptive wavelet technique in comparison to the conventional techniques is that the wavelet coefficients which are used to detect regions with localized features are simply computed by the fast discrete wavelet transform. Therefore, the wavelet based adaptive technique is very fast which is of great importance in time dependent problems in which the mesh should

be repeatedly refined at certain time steps. In contrast, other automatic adaptive techniques are usually based upon the posterior error indicator in which the computation of the posterior indicator often dramatically decreases calculation efficiency.

A short review of the multi-resolution wavelet analysis (MRMA) is given in [15–17]: the mathematical foundation of the adaptive wavelet algorithm is multi-resolution wavelet analysis. The MRWA projects a complicated function into a nested sequence of approximation subspaces $\{V_{j+1}\}$,$V_j \subset V_{j+1}$ and establishes a set of scaling function coefficients a_{jk} and a set of wavelet coefficients d_{jk}, structured over different levels of resolution. Each of subspaces can be decomposed into an approximation space $\{V_j\}$ and its orthogonal complement detail space $\{W_j\}$. The space L^2 can be expanded as an approximation space plus a sum of detail spaces, i.e. $L^2 = V_{j=j0} + \sum_{j=j0} W_j$. The bases of approximation and detail subspaces are constructed with scaled and translated versions of functions $\phi_{j,k}$ and $\psi_{j,k}$ as respectively

$$\{V_j\} = \text{span}\{\phi_{j,k} = 2^{j/2}\phi(2^j x - k)\} \tag{6}$$

$$\{W_j\} = \text{span}\{\psi_{j,k} = 2^{j/2}\psi(2^j x - k)\}, \tag{7}$$

Using $V_j \subset V_{j+1}$ and $W_j \subset V_{j+1}$ we obtain

$$\phi(x) = \sum_k h_k \, \phi(2x - k) \tag{8}$$

$$\psi(x) = \sum_k g_k \, \phi(2x - k). \tag{9}$$

The sequences are respectively low-pass and high-pass filters. The wavelet decomposition of $f(x)$ into $f_j \in V_j$ and $g_j \in W_j$ is

$$f(x) = \sum_k \gamma_{j,k} \, \phi_{j0,k} + \sum_{j=j0} \sum_k \psi_{j,k}. \tag{10}$$

An important point of the wavelet decomposition is the fast discrete wavelet transform (DWT) [18] which provides a simple method of transforming data from one level of resolution j to the coarser level of resolution $j-1$

$$\gamma_{j-1,k} = \sum_l h_{2k-l} \, \gamma_{j,l} \tag{11}$$

$$\kappa_{j-1,k} = \sum_{l} g_{2k-l}\, \kappa_{j,l}. \tag{12}$$

The DWT avoids the unpleasant calculation of the coefficients, γ and κ, which allows the wavelet coefficients to be efficiently calculated using fast numerical convolutions. The scaling function coefficients $\gamma_{j,k}$ present a smoothed version of the function at the current scale, but the wavelet coefficients $\kappa_{j,k}$ present the irregular behaviour of the function (e.g. between the current scale and the next finer scale). At the corresponding level of resolution, the wavelet coefficients are a measurement of the approximation accuracy. The basic idea of the wavelet scheme is to present a function with fewer degrees of freedom while still obtaining an accurate approximation. At any level, the function under analysis is written as a sum

$$f(x) = f^1(x) + f^2(x), \tag{13}$$

where

$$\begin{aligned} f^1(x) = \sum_{k} \gamma_{j0,k}\, \phi_{j0,k} + \sum_{j=j0} \sum_{k} \kappa_{j,k}\, \psi_{j,k} \text{ for } \kappa_{j,k} \geq \eta \\ f^2(x) = \sum_{j=j0} \sum_{k} \kappa_{j,k}\, \psi_{j,k} \text{ for } \kappa_{j,k} < \eta. \end{aligned} \tag{14}$$

The scaling and wavelet coefficients could be obtained from equations (15)

$$\begin{aligned} \gamma_{j,k} &= (f, \phi_{j,k}), \\ \kappa_{j,k} &= (f, \psi_{j,k}). \end{aligned} \tag{15}$$

For a smooth function $f(x)$, the error is bounded by a prescribed threshold $C\eta$ as $|f(x) - f^1(x)| \leq C\eta$, where the parameter C depends on $f(x)$. Further details about the RBF adaptive wavelet method are given in [15, 16]. The extension of the adaptive wavelet method over irregular domain, that is not necessary for our work here, could be found in [17].

The following schematic RBF centers distribution aims to provide readers some insights about the situation we are dealing with (Fig. 1).

It is well known that performance of global RBFs method is very sensitive to both the distribution of points and the selection of RBF shape parameter. In the coming section, we will overview an adaptive technique that allows the global RBFs method to work, *for any shape parameter*, by selecting a proper trial or solution sub-space.

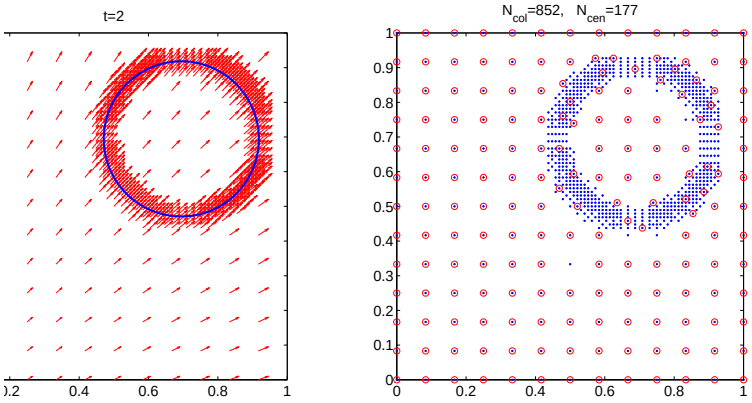

Figure 1: A schematic example of (*Left*) non-uniform node distribution resulted from the wavelet adaptive technique and (*right*) selected RBF centers by the greedy algorithm.

4. Adaptive-globally versus compactly supported RBFs

As seen in Fig. 1, the RBF centers returned from adaptive technique we described just now are highly non-uniform. Such non-unform centers used to bring a lot of difficulties to the global RBF method in which users must determine an appropriate shape parameter. Our answer to this problem is to introduce another level of adaptivity by coupling an adaptive greedy algorithm and wavelet analysis techniques. The proposed method which includes the greedy and wavelet adaptive algorithm is described in this section. Another solution to the non-unform centers is to employ local basis instead of global. Although the shape parameter of CSRBF is still arbitrary, it is commonly accepted fact that this is much less of a problem in comparison to the problem seen in its global counterpart. The numerical methods used in this paper were utilized for the solution of LSM problems either with adaptive MQ RBF or with the CSRBFs. Various examples will then be provided to compare the performances of the choices of basis.

The numerical stability of the global RBF method highly depends on the optimal selection of its centers and the corresponding shape parameters. Intuitively, such optimal locations will depend on many factors: the PDE and its domain, the RBF basis used, the computational precisions, some

user defined parameters, and so on. This makes finding optimal RBF centers and the corresponding shape parameters a very difficult task.

The adaptive greedy algorithm in which the system of equations are partially solved by a series of sub-optimal adaptive greedy algorithms could be used for the selection of nearly optimal subset of RBF centers [19–21]. The idea is to set the $N \times N$ matrix system by chosing N RBF centers and N collocation points. Next, the adaptive algorithm is employed to select an optimal subset of N_p RBF centers. The final approximation is given by the least-squares solution resulting in selection of N_p RBF centers and N collocation points. Some convergence results are given in [22] and recent applications of the method can be found in [23–26]. The selected row and columns are added to the previously selected matrix and the new approximation α_{k+1} is obtained by solving the system associated with $k+1$ collocation points and $k+1$ RBF centers.

Be reminded that the adaptive wavelet techniques produce a dense mesh near the boundaries of moving boundary problems while keeps a relatively coarse mesh elsewhere. The very fine mesh near the boundaries will result in a highly ill conditioned system of equations in which the stable solution is an important issue. On the other side the greedy algorithm starts from finely distributed set of RBF centers and selects a small and nearly optimal subset of it. The greedy adaptive method guaranties that the condition number of resulted system of equations is lower than a prescribed value that ensures stable solution of the system. The first step of adaptive wavelet-greedy technique is to produce a finely distributed RBF centers near the boundaries using the adaptive wavelet procedure described in section 3. The next step is to utilize the adaptive greedy technique, described in section 4, to select nearly optimal RBF centers from the adaptive mesh produced in previous step. The overall procedure of updated RBF collocation method with adaptive wavelet-greedy technique is summarized in Algorithm 1.

5. Numerical results

In the simulations we used the MQ RBF basis $\varphi(r) = \sqrt{r^2 + c^2}$ with shape parameter c and compactly supported RBF spline $\varphi(r) = (1-r)_+^m p(r)$, where $p(r)$ is a polynomial of the Wendland [13] compactly supported (CSRBF) spline:

$$(1-r)_+^m = \begin{cases} p(r), & \text{if} \quad 0 \le r < 1, \\ 0, & \text{if} \quad r \ge 1. \end{cases}$$

Algorithm 1 Wavelet node-refinement with greedy trial space selction

Input data:
Type of RBFs (MQs or CSRBFs, Section 2)
Shape parameter for MQ RBF (Section 2)
Pointer to the greedy (wavelet) method
Initial and boundary conditions
Type of velocity fields (see examples in Section 5)

Initialization:
Generate the base collocation computational grid (e.g. 25×25)
Define the zero contour (as circular bubble, see examples in Section 5)

if the pointer to wavelet method > 0 **then**
Apply the adaptive wavelet method
end if
Iteration:
while $t \leq T_{final}$ **do**
Compute the new zero contour (Section 2)
if the pointer to the wavelet (greedy) method > 0 **then**
Apply the wavelet (greedy) procedure (Section 3 and Section 4)
end if
if the initial contour area $<$ the real contour area **then**
Apply the reinitialization [12]
end if
Solve the problem and calculate the unknown coefficients (Section 2)
Setting time $t := t + \Delta t$
end while

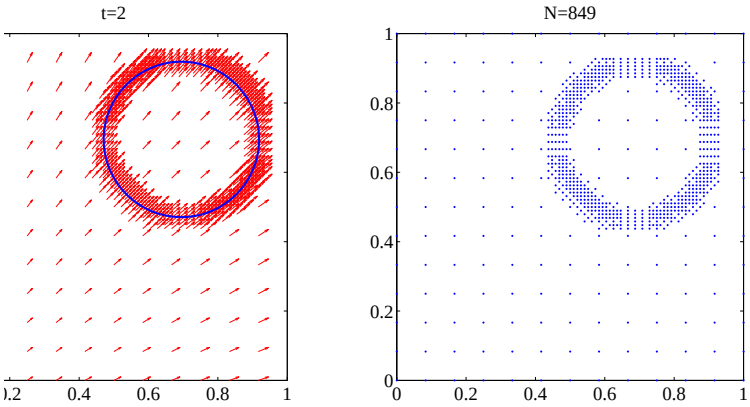

Figure 2: Shape of the interface calculated with the wavelet adaptive CSRBFs method.

5.1. Oriented flow

The first example is a translation of circular interface in oriented flow. The circular bubble of radius $r = 0.15$, initially centered at $(0.3, 0.3)$, moves by the orientated flow in a computational domain of size 1×1 with the velocity field (u, v) defined as follows:

$$u = 0.2(x + 0.5), \tag{16}$$

$$v = 0.2(y + 0.5). \tag{17}$$

Results obtained with the wavelet adaptive RBFs method and greedy algorithm's (see Fig. 1 and Fig. 2) are compared with results obtained in [11]. The results are comparable.

In Fig. 3, the normalized errors [11] of the area as a function of time are presented. The error of the area is calculated for the wavelet adaptive CSRBFs method and the MQ RBFs method and greedy algorithm combination.

5.2. Bubble in a single-vortex flow field

The following examples were also presented in article [27]. First, we consider a circular bubble of radius $r = 0.15$, initially centered at $(0.5, 0.75)$, advecting in a steady, non-uniform vorticity field in a computational domain of size 1×1 with the velocity field (u, v) defined as follows:

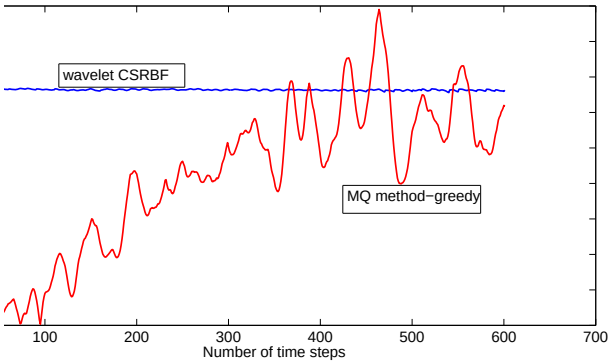

Figure 3: Error of the area at different points in time. Time step is 0.01.

$$u = -\sin^2(\pi x)\sin(2\pi y), \tag{18}$$
$$v = \sin^2(\pi y)\sin(2\pi x). \tag{19}$$

This velocity field possesses vortical flows which deform and possibly tear any interface carried with the flow. In Fig. 4, we can see that the resulting vortex field spins fluid elements, stretching the bubble into long and thin body which spirals around the center of the domain.

Second, we consider a circular bubble of radius $r = 0.25$, initially centered at $(0.5, 0.75)$ in a computational domain of size 1×1 with the velocity field (u, v) defined as follows:

$$u = \sin(4\pi(x + 1/2))\sin(4\pi(y + 1/2)), \tag{20}$$
$$v = \cos(4\pi(x + 1/2))\cos(4\pi(y + 1/2)). \tag{21}$$

The velocity field has the ability to force the bubble to undergo extreme topological changes. The results are presented in Fig. 5.

5.3. Bubble in an advection flow field

Many engineering processes include phase transitions. Computer simulations provide a useful tool for studying such transitions. We consider a circular bubble of radius $r = 0.15$, initially centered at $(0.4, 0.56)$, moved by

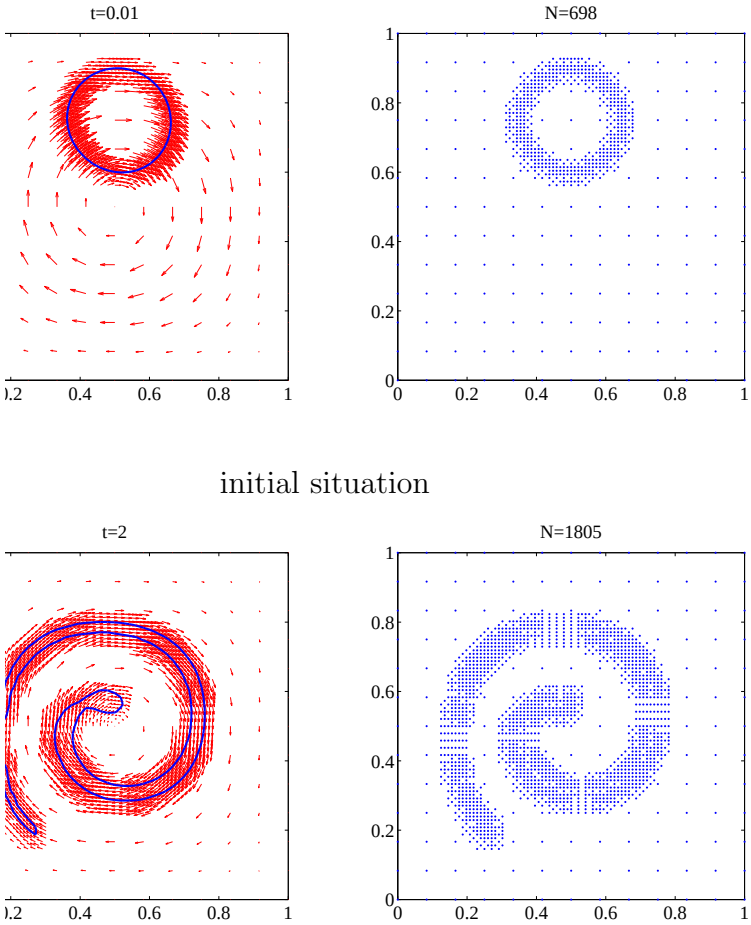

Figure 4: Shape of the bubble in a single-vortex flow field.

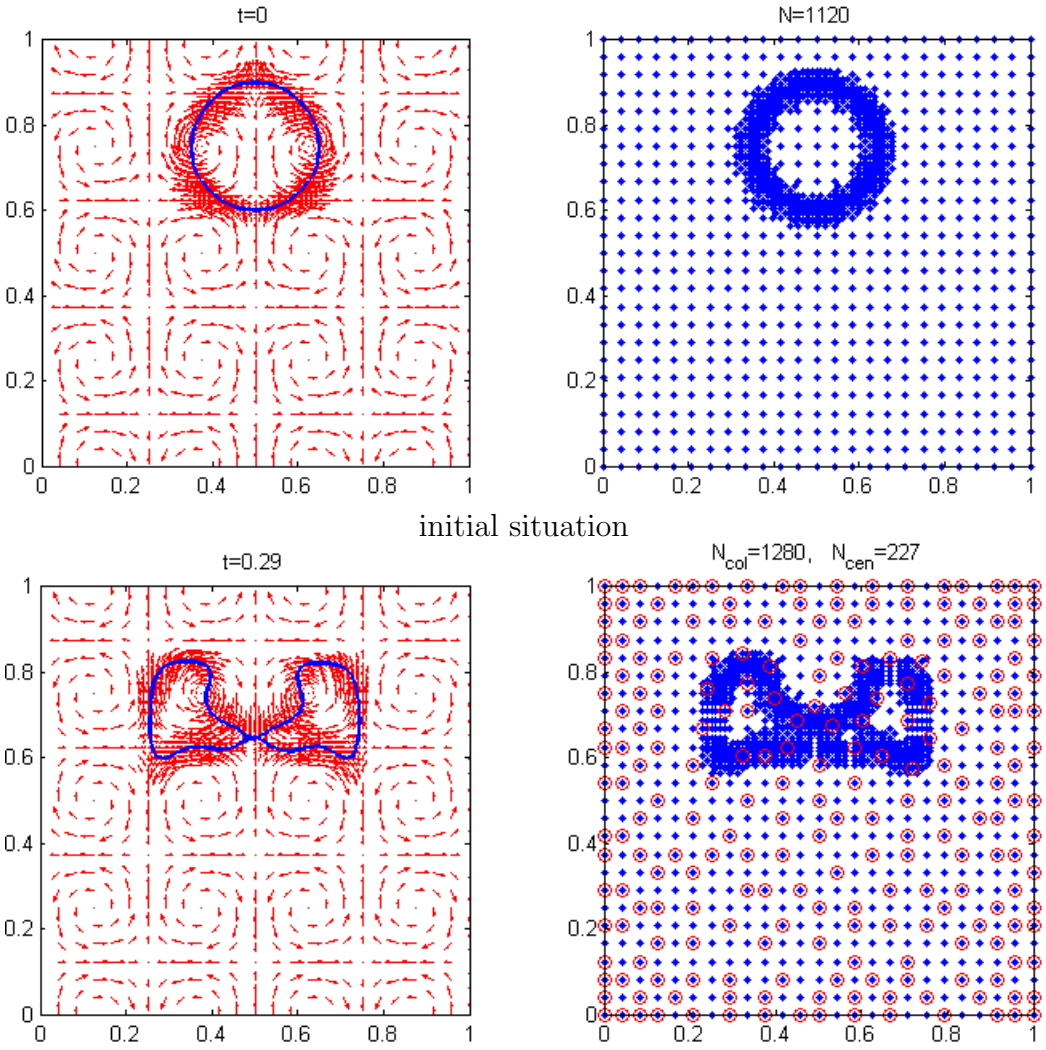

Figure 5: Shape of the bubble in an extreme situation.

a shear flow in a computational domain of size 1×1 with the velocity field (u, v) defined as follows:

$$u = \sin(2\pi x)\sin(2\pi y), \tag{22}$$

$$v = -\cos(2\pi y)\sin(2\pi x). \tag{23}$$

The function Φ is also evaluated on a 49×49 grid in order to find the zero contours. The results are presented in Fig. 6.

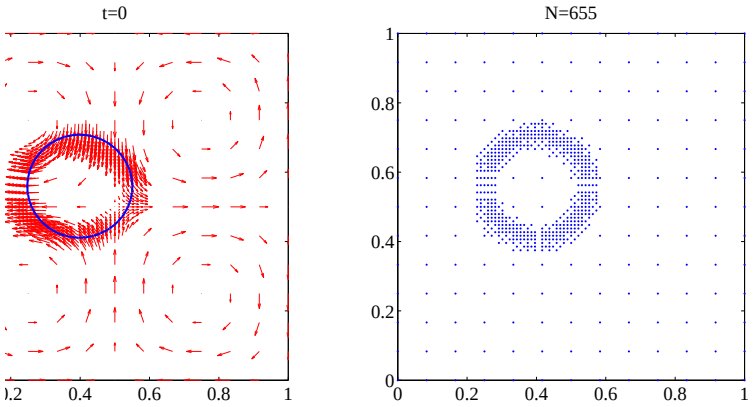

initial situation

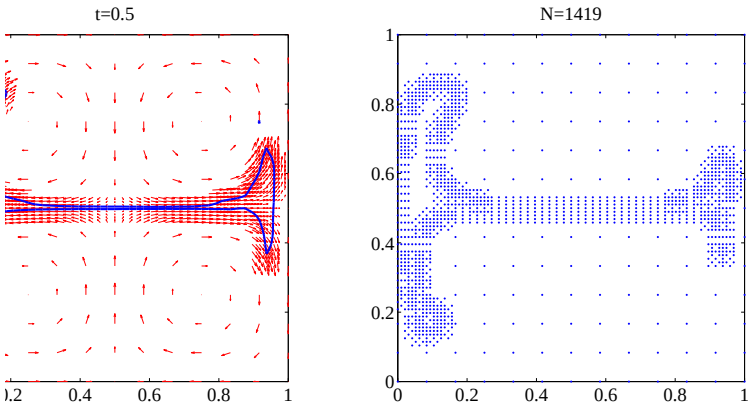

wavelet adaptive CSRBFs method

Figure 6: Shape of the bubble in an advection flow field.

6. Conclusions

This paper outlines the continuation of work done on an alternative approach to the conventional level set methods for solving two-dimensional moving-boundary problems. In this case, the wavelet adaptive RBFs method was added to the earlier approach, which was a combination of MQ RBFs and the adaptive greedy algorithm.

More examples are presented, in particular oriented flow, bubble in a single-vortex flow field and bubble in a advection flow field.

In the conventional level set methods, the level set equation is solved to evolve the interface using a capturing Eulerian approach. The solution procedure requires the appropriate choice of the upwind schemes, reinitialization algorithms and extension velocity methods, which may require excessive amount of computational efforts. In our case, we did some reinitialization in some time steps but the number of required reinitialization has decreased after applying the proposed adaptive techniques. Actually, our examples show that the solutions are much more stable (less artifacts appear in the corners) if the new method (LSM + CSRBF + adaptive wavelet) is employed. The time step was 0.01. We can also conclude that there is instability as the time becomes larger, but the simulations have shown that the instability is less pronounced if the adaptive wavelet CSRBF method was used. This has very beneficial influence on the numerical effectiveness of the method.

Fig. 2 and Fig. 4 show that we can expect more accurate results if the wavelet adaptive RBF method is used. We can clearly emphasize that the greedy-adaptive wavelet method is much more suitable for complicated problems (see Fig. 5 and Fig. 6). In the future work, in the case of greedy algorithms, we are going to check the possible influence of row-weighting for non-uniform grids, but in the case of the CSRBF adaptive method, it is necessary to check if it is possible to implement the method without the adaptive support. We can also conclude that the greedy is developed to work on well-spread but scattered data. Our non-uniform centers requires weighting of some sort.

7. Acknowledgement

This work has been financed by the Slovenian Research Agency (ARRS) through the research program Geotechnology (P0-0268), and Structural mechanics (P2-0260).

References

[1] Crank J. Free and moving boundary problems. Oxford Science Publications. Oxford: Clarendon Press. X, 425 p.; 1984.

[2] Osher S, Fedkiw R. Level set methods and dynamic implicit surfaces. Applied Mathematical Sciences. 153. New York, NY: Springer. xiv, 273 p.; 2003.

[3] Sethian JA. Level set methods and fast marching methods. Evolving interfaces in computational geometry, fluid mechanics, computer vision, and materials science. Cambridge Monographs on Applied and Computational Mathematics. 3. Cambridge: Cambridge University Press. XX, 378 p.; 1999.

[4] Cecil T, Qian JL, Osher S. Numerical methods for high dimensional Hamilton-Jacobi equations using radial basis functions. Journal of Computational Physics 2004; 196:327–347.

[5] Wang S, Wang MY. Radial basis functions and level set method for structural topology optimization. International Journal for numerical methods in Engineering 2006; 65:2060–2090.

[6] Wang SY, Lim KM, Khoo BC, Wang MY. An extended level set method for shape and topology optimization. Journal of Computational Physics 2006; 221:395–421.

[7] Mai-Cao L, Tran-Cong T. A meshless approach to capturing moving interfaces in passive transport problems. CMES Computer Modeling in Engineering & Sciences 2008; 3:157–188.

[8] Javierre E, Vuik C, Vermolen FJ, van der Zwaag S. A comparison of numerical models for one-dimensional Stefan problems. J Comput Appl Math 2006; 192(2):445–459.

[9] Hill JM. One-dimensional Stefan problems: an introduction. Pitman Monographs and Surveys in Pure and Applied Mathematics, 31. Harlow, Essex: Longman Scientific and Technical; New York: John Wiley & Sons, Inc.; XVIII, 204 p.; 1987.

[10] Kansa EJ. Multiquadrics - a scattered data approximation scheme with applications to computational fluid-dynamics. I: Surface approximations and partial derivative estimates. Comput Math Appl 1990; 19(8-9):127–145.

[11] Vrankar L, Kansa EJ, Ling L, Turk G, Runovc F. Moving-boundary problems solved by adaptive radial basis functions. Computers and Fluids 2010; 39:1480–1490.

[12] Osher S, Sethian JA. Fronts propagating with curvature-dependent speed: Algorithms base on Hamilton-Jacobi formulations. J Computational Physics 1988; 79:12–49.

[13] Wendland H. Piecewise Polynomial, Positive Definite and Compactly Supported Radial Basis Functions of Minimal Degree. Advances in Computational Mathematics 1995; 4:389–396.

[14] Daubechies I Orthogonal bases of compactly supported wevelets. Commun Pure Appl Math 1988; 41:225–236.

[15] Libre NA, Emdadi A, Kansa E, Shekarchi M, Rahimian M. A Fast Adaptive Wavelet scheme in RBF Collocation for near singular potential PDEs. CMES:Computer Modeling in Engineering & Sciences 2008; 38(3):263–284.

[16] Libre NA, Emdadi A, Kansa E, Shekarchi M, Rahimian M. A multiresolution prewavelet-based adaptive refinement scheme for RBF approximations of nearly singular problems. Eng Anal Bound Elem 2009; 33:901–914.

[17] Libre NA, Emdadi A, Kansa E, Shekarchi M, Rahimian M. Wavelet based adaptive RBF method for nearly singular poisson–type problems on irregular domains. CMES:Computer Modeling in Engineering & Sciences 2009; 50(2):161–190.

[18] Mallat S. A Wavelet Tour of Signal Processing. Academic Press 1999.

[19] L. Ling, R. Opfer, and R. Schaback. Results on meshless collocation techniques. *Eng. Anal. Bound. Elem.*, 30(4):247–253, 2006.

[20] Ling L, Schaback R. An improved subspace selection algorithm for meshless collocation methods. Int J Numer Methods Eng 2009; 80(13):1623–1639.

[21] Ling L, Schaback R. Stable and convergent unsymmetric meshless collocation methods. SIAM J Numer Anal 2008; 46(3):1097–1115.

[22] T. O. Kwok and Leevan Ling. On convergence of a least-squares Kansa's method for the modified Helmholtz equations. *Adv. Appl. Math. Mech.*, 1(3):367–382, 2009.

[23] L. Ling. An adaptive–hybrid meshfree approximation method. *Int. J. Numer. Methods Eng.*, 89(5):637–657, 2011.

[24] C. S. Chen, T. O. Kwok, and L. Ling. Adaptive method of particular solution for solving 3D inhomogeneous elliptic equations. *Int. J. Compt. Methods*, 7(3):499–511, 2010.

[25] H. Brunner, L. Ling, and M. Yamamoto. Numerical simulations of 2D fractional subdiffusion problems. *J. Comput. Phys.*, 229(18):6613–6622, 2010.

[26] F. L. Yang, L. Ling, and T. Wei. An adaptive greedy technique for inverse boundary determination problem. *J. Comput. Phys.*, 229(22):8484–8496, 2010.

[27] Salih A, Ghosh Moulic S. Some numerical studies of interface advection properties of level set method. Sādhanā 2009; 34(2):271–298.